

Received 17 July 2024; revised 18 August 2024; accepted 28 August 2024; published 30 August 2024

## Sub-GHz Broadband Multi-channel Waveguiding Based on Subwavelength Wire Media

Mykola Khobzei\*

Department of Radio Engineering and Information Security, Yuriy Fedkovych Chernivtsi National University, Chernivtsi, Ukraine

\*Corresponding author (E-mail: m.khobzei@chnu.edu.ua)

**ABSTRACT.** The paper involves the development of a new type of image transfer. With this aim the multi-channel waveguide was considered in a novel representation – it was based on a wire media structure where each space between each four the closest wires is a single subchannel. The utilized wire media (WM) structure has 10-by-10 wires dimensions and 150 mm of the length, thus the first Fabry-Perot resonance appears around 0.9-1 GHz. The goal is to show the broadband multi-channel imaging at frequencies lower than the first Fabry-Perot resonance that means the considered structure tends to electrically short size that has not been studied previously. Taking into account the multi-channel principle of the wire media, the imaging can be performed as a binary one. For this reason, each single channel is fed by individual electromagnetic (EM) source that is a dipole antenna in the non-resonant mode. The reason is to use a weak source and match it with a single channel because in the other case the dipole is perfectly matched at the defined resonance frequency. It was found in the paper that the broadband transfer is possible in the frequency range-under-study and impossible at the region of the first Fabry-Perot resonance due to the perfect complex interaction between all wires of structure. As evidence, a simultaneous transfer of EM power from several independent EM sources shaped as R-letter was performed in the frequency range from 0.3 to 0.75 GHz by simulations and experimental investigations. The clear recovery of the transferred letter is possible in the case when it performs not at the frequency of Fabry-Perot and for the enough value of signal-to-noise ratio (SNR). The binary recovery of the transferred image became possible in the paper with an additional post-image processing with a threshold method involvement.

**KEYWORDS** metamaterials, wire media, imaging, waveguide, broadband.

### I. INTRODUCTION

Over the past twenty years, the development of metamaterials has become one of the most dynamic and exciting areas of scientific research in physics and materials science. Metamaterials, characterized by artificially created structural properties that can grant them with unique electromagnetic properties, have opened new horizons in science and technology. These materials can manipulate electromagnetic waves in ways previously considered impossible, such as negative refraction index, superlenses for subwavelength imaging, and the ability to render objects invisible [1-5].

A special place among various types of metamaterials is occupied by structures based on straight parallelly arranged metallic wires – wire media, which have a range of interesting electromagnetic characteristics, opening new opportunities for the development of modern technologies [6] in the range from microwave to THz and optical frequencies [7-8]. WM consist of periodic arrays of metallic wires that interact with electromagnetic waves, creating an environment with controlled properties. They can provide extremely high electromagnetic permeability and negative values of effective dielectric permittivity, making them promising for applications in fields such as antenna systems, electromagnetic shielding, high-frequency electronics, and image transmission, which will be discussed further [9-11].

WM are well known as tools for energy transmission in narrow and wide frequency ranges; this capability is useful for imaging. This property was first demonstrated in 2005 in

the work [12], and then developed in many other works [13-17]. However, these works studied power and image transmission at Fabry-Perot resonance frequency, which limits the functionality of WM according to its geometric dimensions.

The broadband effect of EM energy transmission was demonstrated in [18] and experimentally confirmed in [19-20]. This opened new possibilities for such applications of WM, including the development of endoscopes, spectrometers, etc. [21], [22]. There were also known works for a binary [23] imaging at Fabry-Perot resonance frequencies, but not broadband.

The broadband effect was first applied for imaging in [11], where the transmission of binary images through an optically long endoscope in the frequency ranges between Fabry-Perot resonances was shown. Image formation was carried out by small EM sources placed at the elementary cells of the WM interface (at the middle position between four adjacent wires). Transmission was simultaneously provided by parallel WM channels, as an analogue of a multi-channel waveguide.

However, the question of the possibility of using this imaging method in a wide frequency range up to Fabry-Perot resonances remains interesting. Thus, I aim to achieve the possibility of digital imaging through WM, which can be proven by simulations and experimentation in the sub-GHz frequency range, where the wavelengths will be much longer than the electrical length of the studied WM.

## II. WIRE MEDIA WAVEGUIDE IMPLEMENTATION AND INVESTIGATION

In [11], we found that each cell (square a-by-a between each 4 the closest wires) of the WM can be used as a separate channel for transmitting EM waves radiated by uncoupled individual point sources. This transmission channel is broadband, allowing the usage of WM as a multi-channel waveguide for binary imaging, with the ability to simultaneously transmit broadband signals or

signals with different frequency values through each channel (as an example, different colours in the optical range).

To assess the unwanted interaction between sources located in adjacent cells, in [11] we studied the resolution of the WM. The period of source placement on the input interface was determined to correctly distinguish them on the output interface. The most accurate was the period of the EM wave source placement area of  $2a$ ; these results will be used in this work.

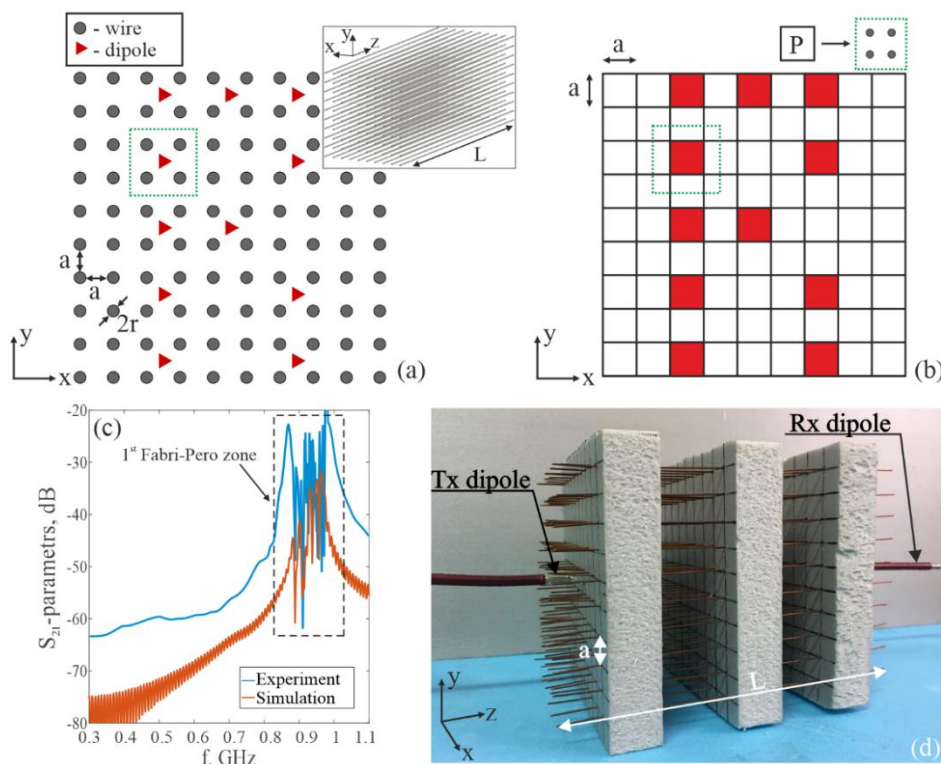


**FIG. 1.** Cross-section XY of the WM model with source locations (red triangles) forming the letter “R” as the transmitted image on the input interface of the WM (a); expected appearance of the detected image on the output interface of the WM (b);  $S_{21}$ -parameter results for simulation and experiment (c); experimental setup for EM signal transmission between two dipole antennas (Tx and Rx) through the WM (d).

Here, I focused on measurements in the sub-GHz frequency range from 0.3 to 1 GHz, so the WM dimensions were chosen as  $L = 150$  mm,  $r = 0.5$  mm, and  $a = 10$  mm, as shown in Figure 1a. A usual electric dipole antenna with a total arm’s length of 10 mm was chosen as an EM signal source for simulations and following experimental measurements. The dipole length was small enough to fit in the WM cell, and the resonance frequencies of these dipoles were significantly higher than the studied frequency range. In CST Microwave Studio, the WM was designed (inset in Figure 1a) with the dimensions described above; perfect electric conductor (PEC) was used as the material for the wires and dipole, the structure was filled with vacuum as the host material, and the time solver was used for simulations. During the experimental measurements, a WM sample was made (Figure 1d) with the same geometric parameters as for the simulations, but the wire material was copper, which has finite conductivity and loss values. The grey material in Figure 1d is used as a holder and is transparent to EM waves of the frequency range-under-study. Two electric dipoles with resonance frequencies significantly higher than the measured

frequency range were made, as in the simulation.

Examining the  $S_{21}$ -parameters shown in Figure 1c, both for the experiment and for the simulation (dipole antennas were placed on the input and output apertures of the WM in the middle of the structure at a distance of 10 mm for better interaction), we observe signal transmission in the wide frequency range of 0.3-1.1 GHz, with the Fabry-Perot resonance frequency range of approximately 0.9-1 GHz clearly visible, as expected for the used length  $L$  of wires. One can also clearly see the operating frequency range from  $\sim 0.3$  to  $\sim 0.9$  GHz, which is of interest for our image transmission study.

Based on the results obtained above regarding the operating frequency range, the transmission of the letter “R” was performed as shown in Figure 1a. Dipole sources were arranged with a period of no less than  $2a$ , as was found in the previous studies [11], along the X and Y axes, thus one image pixel had a size of  $2a$  by  $2a$ , as shown in the inset in Figure 1b (green dashed square). Ideally, it was expected to detect maximum power values at the points corresponding to the Tx source positions on the receiving side of the WM, as shown in Figure 1b.

The E-field distribution was obtained using simulations in the XY-plane cross-section at a distance of 10 mm from the input interface inside the WM ( $Z = 10$  mm). The results are presented in Figure 2 for frequencies [300:50:750] MHz. Consequently, clear images that can be recognized at the output interface were obtained for the range from ~400 to 700 MHz (Figure 2b-i). The E-field distribution in Figure 2a and j is unclear. The indistinct reproduction at

the lowest frequencies is related to the low power that can be transferred to the Rx dipole as is seen from Figure 1c, where  $S_{21}$ -parameters spectrum is around -60...-80 dB – a very low SNR. For the highest frequencies – 750 MHz and more, the reason on worth recognition is the closeness to the first Fabry-Perot resonance where all wires become resonant and their interaction is much stronger than for the operation at the frequencies far from the Fabry-Perot case.

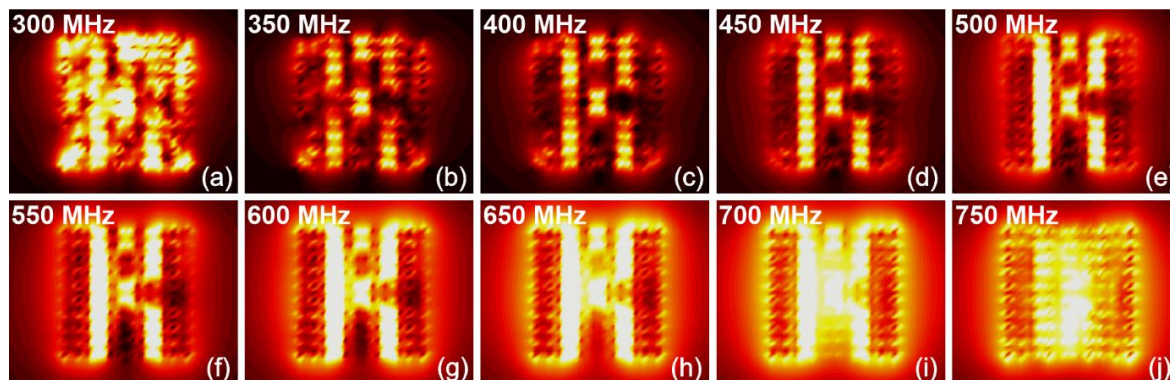


**FIG. 2.** The results of simulations for E-field distributions at the output interface as a cross-section at XY-plane for  $Z = 140$  mm at the frequencies [300:50:750] MHz for letter “R” transfer as a digital picture.

For experimental measurements, we used the same experimental setup shown in Figure 1d, and the sources arranged as in Figure 1a. The same conventional 10 mm electric dipoles (resonance completely exceeds the studied frequency range) were used as sources. I used one Tx dipole and one Rx dipole. The position of the Tx dipole was changed according to the positions in Figure 1a. The Rx dipole scanned the entire XY plane for  $Z = L - 10 = 140$  mm with a discrete step  $a$  (in the center of each cell) for each of the 11 positions. For visualization, all scanned Rx antenna distributions were combined by the principle of superposition and analyzed. Thus, the experimental results are shown in Figure 3 as E-field distributions for frequencies [400:50:750] MHz. It can be seen that the

recognition of the letter “R” is possible in the range from 500 to 700 MHz (Figure 7c-d) and not possible at other frequencies.

The preliminary results are presented as a continuous E-field distribution, but our ultimate goal is the digital recovery of the transmitted binary image. Therefore, the digital post-image processing was applied for an analysis of the previously obtained E-field distributions using a threshold method. The floating threshold value was selected to achieve the best distribution of the discrete points, and as a result, we obtained images as shown in Fig. 4. It can be seen that the obtained results confirm the operating frequency range from 500 to 700 MHz (Figure 8c-d), which accounts for more than 30% of the band.

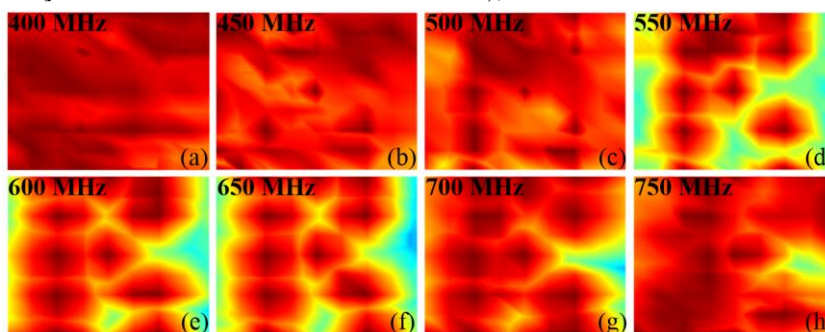


**FIG. 3.** The experimentally obtained E-field distributions for the transfer of digital image for letter “R”.

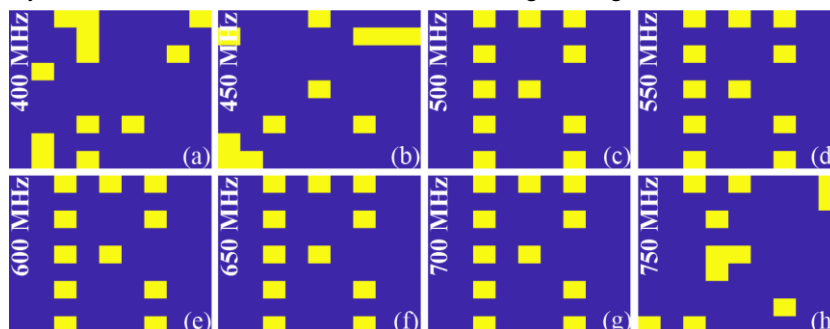


**FIG. 4.** The recognized at the output interface transferred discrete image (“R” letter) after simple digital post-processing.

### III. CONCLUSION

This investigation has successfully demonstrated the ability to transmit multiple harmonic signals through a wire media structure over a wide frequency range (500-700 MHz, constituting more than 30% of the bandwidth) using an array of dipole sources. Through simulations and experimental studies, we confirmed the broadband signal transmission effect, which enhances the device's functionality.

The implications of these results extend to the fields of endoscopy and spectroscopy, where it is crucial not only to detect particles but also to determine their shape and distribution, thereby expanding detection methods through power transfer. The discretized WM interface proposed in this study meets these requirements.

In the sub-GHz microwave frequency range, the investigated structure shows potential for application in multichannel waveguides, facilitating the transmission of harmonic and broadband signals. Although the use of such endoscopic devices faces greater challenges in the sub-THz/THz and optical ranges, our results remain relevant and applicable.

I believe that the technical insights and methodologies developed in this work will significantly contribute to the advancement of WM research and improve detection capabilities in related applications.

### ACKNOWLEDGMENT

In this section, I would like to express my gratitude to Dr. Dmytro Vovchuk for his consultation on this article and for his years of academic assistance and scientific support.

### AUTHOR CONTRIBUTIONS

M.K. – conceptualization, methodology, investigation; writing (original draft preparation), writing (review and editing).

### COMPETING INTERESTS

The author declare no competing interests.

### REFERENCES

- [1] Smith, D. R., Pendry, J. B., & Wiltshire, M. C. K. (2004). Metamaterials and Negative Refractive Index. *Science*, 305(5685), 788-792.
- [2] Soukoulis, C. M., & Wegener, M. (2011). Past achievements and future challenges in the development of three-dimensional photonic metamaterials. *Nature Photonics*, 5(9), 523-530.
- [3] N. I. Zheludev and Y. S. Kivshar, "From metamaterials to metadevices," *Nat. Mater.*, vol. 11, no. 11, pp. 917–924, 2012.
- [4] C. Della Giovampaola and N. Engheta, "Digital metamaterials," *Nat. Mater.*, vol. 13, no. 12, pp. 1115–1121, 2014.
- [5] T. J. Cui, M. Q. Qi, X. Wan, J. Zhao, and Q. Cheng, "Coding metamaterials, digital metamaterials and programmable metamaterials," *Light Sci. Appl.*, vol. 3, no. 10, pp. e218–e218, 2014.
- [6] C. R. Simovski, P. A. Belov, A. V. Atrashchenko, and Y. S. Kivshar, "Wire metamaterials: physics and applications," *Adv. Mater.*, vol. 24, no. 31, pp. 4229–4248, 2012.
- [7] O. T. Naman *et al.*, "Indefinite media based on wire array metamaterials for the THz and mid-IR," *Adv. Opt. Mater.*, vol. 1, no. 12, pp. 971–977, 2013.
- [8] S. Hrabar, "Application of wire media in antenna technology," in *Metamaterials and Plasmonics: Fundamentals, Modelling, Applications*, Dordrecht: Springer Netherlands, 2008, pp. 139–151.
- [9] D. Vovchuk and M. Khobzei, "Investigation of frequencies characteristics of modified waveguide aperture by wire media," *Prog. Electromagn. Res. Lett.*, vol. 93, pp. 59–64, 2020.
- [10] P. Robulets, D. Vovchuk, M. Khobzei, Y. Derevesnikova, M. Apostolyuk, and L. Politanskyi, "Multiple harmonic signal transfer using wire media structure," in *2020 IEEE 15th International Conference on Advanced Trends in Radioelectronics, Telecommunications and Computer Engineering (TCSET)*, 2020.
- [11] D. Vovchuk, M. Khobzei, M. Apostoliuk, V. Tkach, and C. Simovski, "Broadband transfer of binary images via optically long wire media," *Nanophotonics*, vol. 12, no. 14, pp. 2797–2807, 2023.
- [12] P. A. Belov, C. R. Simovski, and P. Ikonen, "Canalization of subwavelength images by electromagnetic crystals," *Phys. Rev. B*, vol. 71, no. 19, p. 193105, May 2005, doi: 10.1103/PhysRevB.71.193105.
- [13] P. A. Belov and Y. Hao, "Subwavelength imaging at optical frequencies using a transmission device formed by a periodic layered metal-dielectric structure operating in the canalization regime," *Phys. Rev. B*, vol. 73, no. 11, p. 113110, Mar. 2006, doi: 10.1103/PhysRevB.73.113110.
- [14] P. A. Belov, Y. Hao, and S. Sudhakaran, "Subwavelength microwave imaging using an array of parallel conducting wires as a lens," *Phys. Rev. B*, vol. 73, no. 3, p. 033108, Jan. 2006, doi: 10.1103/PhysRevB.73.033108.
- [15] I. S. Nefedov, X. Dardenne, C. Craeye, and S. A. Tretyakov, "Backward waves in a waveguide, filled with wire media," *Microw. Opt. Technol. Lett.*, vol. 48, no. 12, pp. 2560–2564, 2006.
- [16] X. Radu, A. Lapeyronnie, and C. Craeye, "Numerical and experimental analysis of a wire medium collimator for magnetic resonance imaging," *Electromagnetics*, vol. 28, no. 7, pp. 531–543, 2008.
- [17] K. J. Kaltenecker *et al.*, "Ultrabroadband perfect imaging in terahertz wire media using single-cycle pulses," *Optica*, vol. 3, no. 5, p. 458, 2016.
- [18] I. S. Nefedov and C. R. Simovski, "Giant radiation heat transfer through micron gaps," *Phys. Rev. B*, vol. 84, no. 19, p. 195459, Nov. 2011, doi: 10.1103/PhysRevB.84.195459.
- [19] D. Vovchuk, S. Kosulnikov, I. Nefedov, S. Tretyakov, and C. R. Simovski, "Multi-Mode Broadband Power Transfer through a Wire Medium Slab (Invited Paper)," *Prog. Electromagn. Res.*, vol. 154, pp. 171–180, 2015, doi: 10.2528/PIER15111908.
- [20] S. Kosulnikov, D. Vovchuk, I. Nefedov, S. Tretyakov, and C. Simovski, "Broadband power transfer through a metallic wire medium slab," *2016 URSI Int. Symp. Electromagn. Theory, EMTS 2016*, pp. 594–597, Sep. 2016, doi: 10.1109/URSI-EMTS.2016.7571463.
- [21] C. Simovski, D. Vovchuk, and S. Kosulnikov, "Unusual eigenmodes of wire-medium endoscopes: impact on transmission properties," *Opt. Express*, Vol. 26, Issue 14, pp. 17988–18005, vol. 26, no. 14, pp. 17988–18005, Jul. 2018, doi: 10.1364/OE.26.017988.
- [22] X. Radu, D. Garray, and C. Craeye, "Toward a wire

medium endoscope for MRI imaging,” *Metamaterials*, vol. 3, no. 2, pp. 90–99, Oct. 2009, doi: 10.1016/J.METMAT.2009.07.005.

- [23] A. Ono, J. Kato, and S. Kawata, “Subwavelength Optical Imaging through a Metallic Nanorod Array,” *Phys. Rev. Lett.*, vol. 95, no. 26, p. 267407, Dec. 2005, doi: 10.1103/PhysRevLett.95.267407.



### Mykola Khobzei

PhD student at Radio Engineering and Information Security Department of Yuriy Fedkovych Chernivtsi National University. Research field includes wire metamaterials for the transmission and radiation, radar detection and sensors. Author of more than 20 publications.

ORCID ID: 0000-0002-9101-8569

## Суб-ГГц широкопasmовий багатоканальний хвилевід на основі напівхвильового середовища із провідників

Микола Хобзей\*

Кафедра радіотехніки та інформаційної безпеки, Чернівецький національний університету імені Юрія Федьковича, Чернівці, Україна

\*Автор-кореспондент (Електронна адреса: m.khobzei@chnu.edu.ua)

**АНОТАЦІЯ** У статті розглядається розроблення нового типу передавання зображень. З цією метою було досліджено багатоканальний хвилевід у його новому представленні – на основі структури з паралельних провідників (СПП), де кожен простір між чотирма найближчими провідниками утворює окремий передавальний канал. Використана СПП має розмірність 10 на 10 провідників і довжину 150 мм, тому перший резонанс Фабрі-Перо спостерігається в діапазоні частот 0.9-1 ГГц. Метою дослідження є передавання зображень в широкому діапазоні частот, яке формується на вхідній апертурі СПП-хвилевода на частотах нижче першого резонансу Фабрі-Перо. Це означає, що розглянута структура має електрично малий розмір в порівнянні з довжиною хвилі, що раніше не досліджувалося. Враховуючи багатоканальний принцип розглядуваного хвилевода, зображення може бути відновлено в бінарному форматі на приймальній стороні. Для цього кожен окремий канал живиться окремим електромагнітним (ЕМ) джерелом, яке являється дипольною антеною в нерезонансному режимі. Це дозволяє використовувати слабе ЕМ джерело і узгоджувати його з окремим каналом, оскільки в іншому випадку диполь ідеально узгоджений на визначеній резонансній частоті і здійснює випромінювання незалежно від наявності СПП. У статті було встановлено, що широкопasmове передавання зображення можливе в досліджуваному частотному діапазоні і неможливе в області першого резонансу Фабрі-Перо через взаємодію між усіма провідниками структури одночасно. Як доказ, було проведено одночасне передавання ЕМ енергії від кількох незалежних ЕМ джерел у вигляді літери "R" у частотному діапазоні від 0.3 до 0.75 ГГц за допомогою моделювання та експериментальних досліджень. Чітке відновлення переданої літери стало можливим, коли це відбувалося на частотах, відмінних від частоти резонансу Фабрі-Перо, та за умови достатнього значення відношення сигнал/шум. Бінарне відновлення переданого зображення стало можливим завдяки додатковому аналізу отриманих сигналів зображення, де в алгоритмі використовувався метод порівняння з пороговим значенням.

**КЛЮЧОВІ СЛОВА** метаматеріали, структури з паралельних провідників, зображення, хвилевід, широкопasmовість.



This article is licensed under a Creative Commons Attribution 4.0 International License. To view a copy of this licence, visit <http://creativecommons.org/licenses/by/4.0/>.